Dyes and Pigments 91 (2011) 396–403

Contents lists available at ScienceDirect

Dyes and Pigments

journal homepage: www.elsevier.com/locate/dyepig

Thermochromic behavior ($400 < T\,^{\circ}C < 1200\,^{\circ}C$) of barium carbonate/binary metal oxide mixtures

E. Lataste [a], A. Demourgues [a], J. Salmi [b], C. Naporea [b], M. Gaudon [a,*]

[a] CNRS, Université de Bordeaux, ICMCB, 87 avenue du Dr. A. Schweitzer, Pessac F-33608, France
[b] Marion Technologies S.A., Parc Technologique Delta Sud, 09340 Vernolle, France

ARTICLE INFO

Article history:
Received 8 November 2010
Received in revised form
16 May 2011
Accepted 16 May 2011
Available online 23 May 2011

Keywords:
Inorganic pigments
Thermochromism
Metal oxides
Barium carbonates
Colour
Bond Valence

ABSTRACT

Irreversible thermochromism over a wide temperature range has been observed from the decomposition of a mixture of a barium carbonate and a metal oxide. The control of the reaction temperature can be predicted from the calculation of the Madelung energy of the barium/transition metal mixed oxide formed consecutively with the decarbonatation. Moreover, the Madelung energy of this formed mixed oxide may be predicted from bond valence considerations. This study offers a simple predictive approach to propose temperature indicators with significant optical contrast and a thermochromic temperature varying between 400 and 1200 °C.

1. Introduction

Currently, thermochromic materials receive much attention due to their potential applications as user friendly temperature indicators [1–5] in a wide range of devices such as aeronautic motors, chill-checkers, cooking tools, hotplates and furnaces. Thermochromic materials can be defined as materials presenting either a reversible or irreversible color change with respect to temperature [6,7]. Irreversible change of colors over a wide range of temperature can be reached by the decomposition of inorganic materials as phosphates, carbonates and hydroxides. Decomposition reactions of such inorganic compounds can be written as:

$$A(s) \rightarrow B(s) + \text{gases}.$$

An example of one solid decomposition following this reaction pattern is the decomposition of some alkaline-earth (Ca, Sr, Ba) carbonates as described by equation (1):

$$ACO_3\,(s) \rightarrow AO\,(s) + CO_2\,(g). \qquad (1)$$

Such a reaction can be coupled with another transition metal oxide reagent with the aim of forming a mixed oxide, as described in the following reaction (2):

$$y\,ACO_3\,(s) + z\,B_xO\,(s) \rightarrow A_yB_{zx}O_{y+z}\,(s) + y\,CO_2\,(g). \qquad (2)$$

The control of the latter reaction temperature is of interest since a thermochromic phenomenon [8] can be associated with this decomposition. Indeed, the formed mixed oxide has a different color from the reagent oxides, demonstrating an irreversible thermochromic effect. Using barium carbonates, the reaction (2) takes place whatever the transition metal cation used, since $Ba_yB_{zx}O_{y+z}$ mixed oxides are generally more stable than the BaO simple oxide.

In a ionic model approach, the reticular energy of a solid (or lattice binding energy, hereafter named Er) corresponds to the required energy for complete separation of one mole of a solid ionic compound into its ionic components in the gaseous state (ex: AO $(s) \rightarrow A^{2+}(g) + O^{2-}(g)$). The higher the reticular energy, the higher the crystal stability is. Experimentally, the reticular energy can be calculated from Born–Haber–Fajans cycles using calorimeters. Nevertheless, if one knows the structure and the composition of an ionic compound, various electrostatic models in which the energy is a function of the distances between anions and cations inside the crystal framework can be used to directly determine the solid reticular energy. Here, the Madelung term of the Born–Lande

* Corresponding author.
E-mail address: gaudon@icmcb-bordeaux.cnrs.fr (M. Gaudon).

0143-7208/$ – see front matter © 2011 Elsevier Ltd. All rights reserved.
doi:10.1016/j.dyepig.2011.05.016

Table 1
Mixed oxides formed after annealing at 1100 °C. The % is relative to an approximated content assimilated to the main peak relative intensity of each phase on the X-ray diffractograms.

	Reagents		Products (1100 °C)					
			Formed mixed oxides				Reagents excess	
	$BaCO_3$	Fe_2O_3	$BaFe_{12}O_{19}$	$BaFe_4O_7$	$BaFe_2O_4$	$BaFeO_{3-x}$	$BaCO_3$	Fe_2O_3
A	38 wt%	62 wt%	24%	0%	21%	3%	36%	16%
B	80 wt%	20 wt%	2%	1%	3%	68%	26%	0%
C	98 wt%	2 wt%	0%	0%	3%	3%	94%	0%

equation was considered in this work as an approximation of the reticular energy [9].

From a thermodynamic point of view, equations (1) and (2) are linked to the Madelung reticular energies of each solid compound and the formation energy (ΔG_f) of the y moles of gaseous carbon dioxide. The temperature of the reaction is inversely proportional to the difference between the starting compounds energies and the product energies: ΔE. Considering the reactivity of cations with carbonates is strongly dependent upon their electronegativity, the lower the A^{2+} cations electronegativity is, higher the cations affinity for large covalent anionic ligands like CO_3^{2-}. Furthermore, simple AO oxides have reticular energy increasing versus A^{2+} electronegativity. Thus, focusing on the A^{2+} alkaline-earth ions for which their electronegativity decreases with their increase in atomic number, $MgCO_3$ carbonate is less stable than $SrCO_3$, the latter being less stable than $BaCO_3$ [10]. In a first approximation, thermochromic decomposition with tunable temperature can be imagined considering that higher the Er_3 energy (reticular energy of the mixed oxide formed after decarbonatation), the higher the ΔE of the decomposition reaction, the lower the reaction temperature (T_D) is. Considering the large choice of the initial metal oxides which can be used (large choice of B^{2+} cations), such reactions can lead to thermal indicators with significant color variation enabling one to follow a wide range of temperature changes. Hence, thermochromic paints which can be obtained from the chemical reaction of an alkaline-earth carbonates and a transition metal oxide are highly attractive.

In the first part of this paper, the decarbonatation reaction has been conducted with an initial mixture containing barium carbonate $BaCO_3$ and hematite Fe_2O_3 as the additive oxide. The sudden color change of this mixture from red to black allowed the study of the decarbonatation reaction parameters (relative quantity of barium carbonate and hematite). Several techniques were used for identifying the decarbonatation temperatures and mechanism: spectrophotometry to characterize the colorimetric changes, X-ray diffraction for structural studies and thermogravimetric analyses (TGA) to determine the mass loss associated with the decomposition. In the second part, various binary and ternary oxides have been tested with the aim of varying the decarbonatation temperature for expanding industrial applications. In a last part of this study, the correlation between decarbonatation temperatures and the Madelung energy of the ternary oxides formed after decarbonatation (Er_3) has been established. This feature allows the prediction of the operational temperature of the other thermochromic alkaline-earth carbonate/binary metal oxide mixtures abilities (approximation of the temperature of the thermochromic colour change).

2. Experimental section

The starting thermochromic mixtures were prepared by grinding in an agate mortar one carbonate powder with one binary/ternary oxide powder. The starting materials were purchased from either Aldrich (MoO_3, Co_3O_4, ZnO, Cu_2O, NiO, Bi_2O_3, Cr_2O_3), Prolabo ($BaCO_3$), BDH (WO_3) or Merck (α-Al_2O_3, V_2O_5). The complex oxides herein tested were synthesized from these raw products by solid-state reaction at high temperature performed in our laboratory ($CuMoO_4$, $CoAl_2O_4$, Fe_2O_3, ZnO:Co, $Y_2Ti_2O_7$).

The decomposition reaction advancement versus temperature has been studied. The thermal treatment dwell is fixed to five min. at the desired temperature ($400\ °C \leq T \leq 1200\ °C$), the powder is then quenched to room temperature.

2.1. X-ray diffraction

X-Ray Diffraction (XRD) measurement was carried out at room temperature in the $10° \leq 2\theta \leq 80°$ range (step 0.017°) on a PANalytical X'PERT PRO diffractometer equipped with X'Celerator detector mounted in Bragg-Brentano scattering geometry. CuKα (Kα_1-Kα_2) radiation was used as X-Ray source.

2.2. Spectrophotometry

Visible-NIR spectroscopy analyses were carried out in Diffuse Reflectance mode with a KONICA-MINOLTA CM-700d spectrophotometer equipped with an integrating sphere coated with polytetrafluoroethylene (PTFE). Measurements were performed for wavelengths varying from 200 nm up to 800 nm, in Specular Component Excluded (SCE) mode. A white calibration cap CM-A177 (ceramic) was used as the white reference and the standard D65 (Daylight, color temperature: 6504 K) with a 10° observer angle (CIE1964) as illuminant. Only the UV–visible wavelength range and the La^*b^* space parameters (L: luminosity, a^*: green to red axis and b^*: yellow to blue axis coefficients) are discussed in this paper. L luminosity can be assimilated to grey level defined on a hundred graduation scale. No mathematical treatment has to be conducted since the apparatus directly gives La^*b^* chromatic parameters. The optical contrast (OC) between two colors corresponds to the distance between the coordinates of these two colors in the La^*b^* space, such as $OC^2 = \Delta L^2 + \Delta a^2 + \Delta b^2$.

Table 2
Representation of the colors (La^*b^* parameter) and optical contrasts between two consecutive colors of the three A, B, C mixtures after annealing at various temperatures between 700 °C and 1200 °C.

	700°C	OC	800°C	OC	900°C	OC	1000°C	OC	1100°C	OC	1200°C
A	36.0 29.3 19.9	1.4	35.629 .6 21.2	3.2	37.8 28.9 23.2	16.8	33.1 15.0 15.0	10.3	29.9 6.7 10.0	13.5	33.1 0.7 -1.6
B	39.9 27.6 17.4	7.2	39.5 27.8 24.5	29. 5	33.5 2.7 10.3	17.9	18.94 -0.06 0.41	0.7	19.57 -0.25 0.21	1.7	20.8 0.0 1.3
C			66.7 11.4 10.2	21	51.5 0.7 0.3	12.3	49.8 3.2 12.3	6.5	48.5 1.4 6.2		

2.3. Thermogravimetric analyses

A Setaram MTB 10-8 system was used for recording the thermogravimetric curves of the carbonates – metal oxides mixtures. The experiments were carried out under an oxygen flow (180 mL min^{-1}) in corundum crucibles containing around 40 mg of sample with a constant heating rate of 3 K min^{-1} up to 1250 °C.

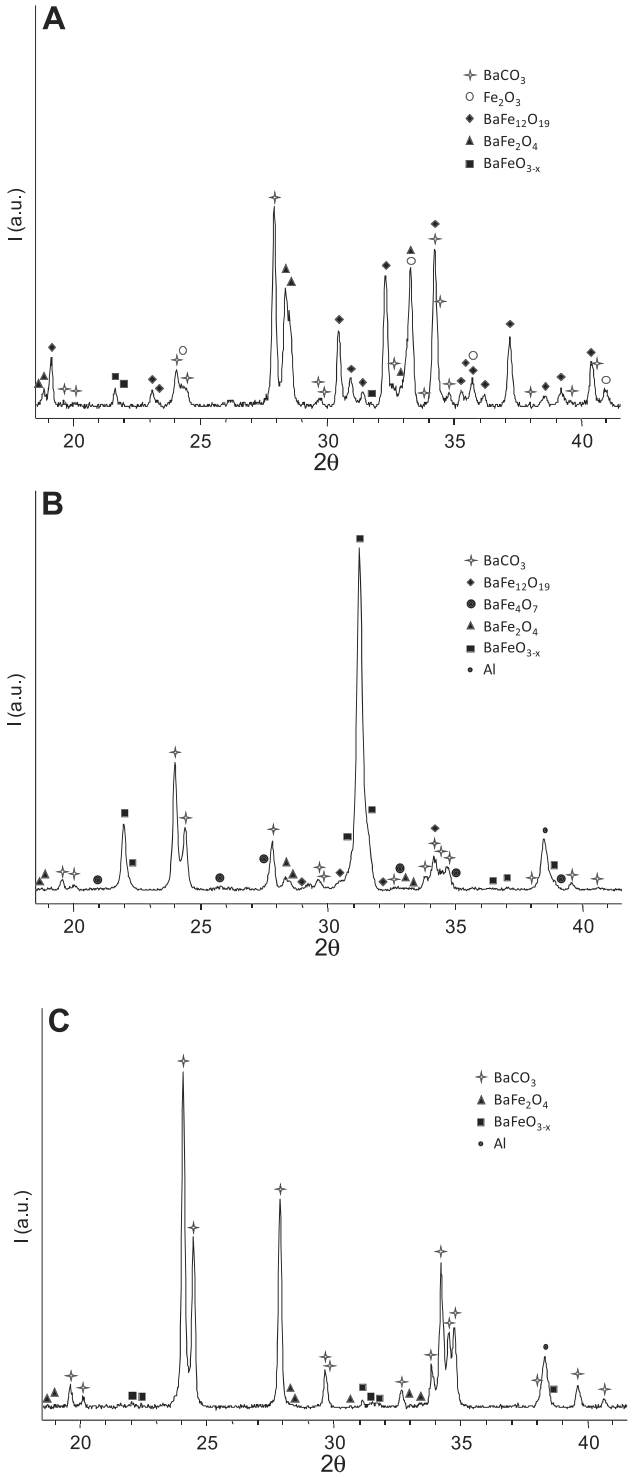

Fig. 1. X-ray diffractograms of the three A, B, C mixtures containing various weight contents of $BaCO_3$ and Fe_2O_3 and annealed at 1100 °C.

2.4. Madelung term of the reticular energies calculation

The Madelung term of the reticular energies is hereafter calculated using an ionic model approach derived from Madelung Theory. This theory, based on a point charge model (formal charge considering a purely ionic system), takes into account the potential of every site of the crystal lattice in order to respect the oxidation degree of each element. The calculation of the reticular energies was made using a program developed in 1990 based on the Ewald approximation [11] (Ewald summation). For each calculation, this program requires the complete crystal structure parameters, i.e., the lattice parameters and the ion positions. The Ewald summation allows only the calculation of the Madelung term of the reticular energies; the repulsive contribution is not taken into account. Hence the reticular energies here proposed are both systematically slightly over-estimated in comparison to the reticular energies which can be found in the literature and issued from more complex models or Born–Haber–Fajans cycles.

3. Results and discussion

3.1. Investigation of the decomposition of $BaCO_3$–Fe_2O_3 mixtures

Hematite – iron III oxide Fe_2O_3 (α-polymorph) – is the more common red pigment. The oxide crystallizes in a rhombohedral symmetry with an *R-3c* space group deriving from a hexagonal pack of oxygen anions in which 2/3 of the octahedral sites are filled with Fe^{3+} ions.

In this first part, the objective is to understand the effect of carbonate/oxide ratio on the decarbonatation reaction. Thus, various barium carbonate mole percentages in the starting mixture were tested. The results obtained on three characteristic mixtures leading to different ternary main oxides, are reported in Table 1; from A to C, mixtures are composed of an increasing amount of barium carbonate.

From a colorimetric point of view, the mixtures quenched at temperatures between 700 °C and 1200 °C show a color change from red to black (or grey) with optical contrast and temperature ranges both depending on the carbonate/oxide ratio (Table 2). Indeed, a color change starts at about 950 °C for mixture A whereas it is detected at ca. 850 °C for mixtures B and C. The higher the

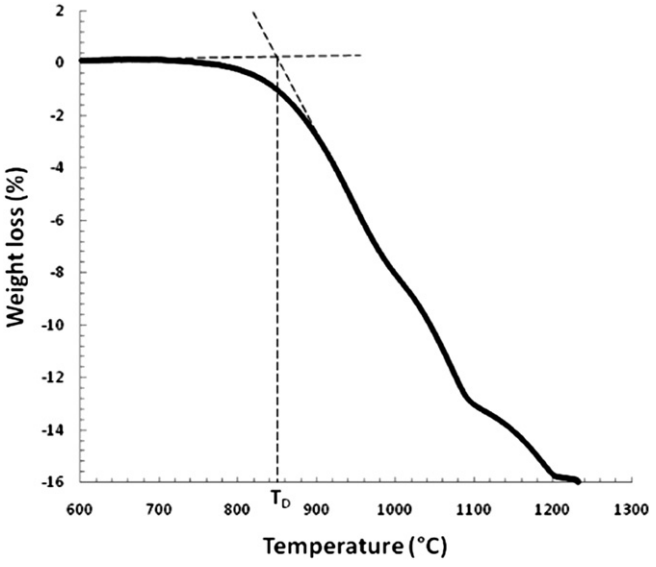

Fig. 2. Thermogravimetric analysis under air atmosphere on the B mixture.

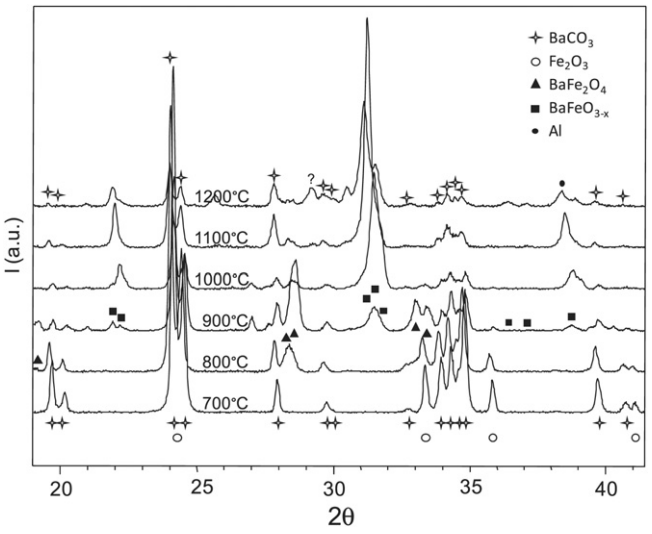

Fig. 3. X-ray diffractograms of B mixture annealed at temperatures ranging between 700 °C and 1200 °C.

content of carbonate in the initial mixture is, the lower the color change temperature (thermochromic effect). At this point, two causes for the thermochromic temperature dependence on the hematite/$BaCO_3$ proportions can be proposed: (i) an effect of the pigment dilution: the lower is the pigment content, the more sensitive the color of the mixture is to its disappearance, (ii) the formation of various mixed oxides (with various coloration and different formation temperatures) depend on the starting mixture composition.

An analysis by X-ray diffraction was performed on the A, B and C mixtures quenched at 1100 °C with the aim of identifying the formed phases. The diffractograms of these three quenched decarbonatation mixtures are reported in the Fig. 1. The X-Ray diffraction results confirm that the reaction between the carbonate and the oxide, as predicted by thermodynamics, leads to the formation of mixed oxides containing both barium and iron cations. However, some differences appear in the formed phases depending on the starting carbonate/oxide ratio. Indeed for low carbonate and high oxide content in the initial mixture (mixture A), reaction between carbonate and oxide is not total and the oxide is only partially consumed: the main phase at 1100 °C is due to remaining $BaCO_3$ and a minor fraction of hematite. Besides the main phase, three different mixed oxides are formed: $BaFe_{12}O_{19}$, $BaFe_2O_4$ and $BaFeO_{3-x}$ in decreasing proportions. Mixtures B and C with a higher content of carbonate and a lower content of oxide than the A mixture, lead after decarbonatation to a complete consumption of the hematite reagent. The main formed phases are the $BaFe_2O_4$ and $BaFeO_{3-x}$ type-phases which are obviously the ones with the highest Ba/Fe ratios. This phenomenon explains the various decomposition temperatures observed depending on the starting Ba/Fe ratio. It is suggested that $BaFe_2O_4$ and $BaFeO_{3-x}$ type-phases are more stable (stronger reticular energy) than the $BaFe_{12}O_{19}$ oxide. Moreover, the formation of various mixed oxide species also explains the different colors (various grey levels) of the final mixture between the three mixtures quenched at the same temperature. Considering that both the main iron mixed oxides formed: $BaFeO_{3-x}$ and $BaFe_2O_4$, are black due to the intervalence electronic transitions between the various iron oxidation states (Fe^{3+} and Fe^{4+}), the grey level which is darker from A to C and B mixtures (see the L luminosity parameter of the three samples obtained after decarbonatation, Table 2), can be interpreted as the consumption of the $BaCO_3$ reagent becoming more important, in this order. The change of color between the reagent mixture and formed mixed oxide is due to the increase of the oxidation state of the Fe transition metal while it is associated to Ba^{2+} in a ternary oxide in comparison to the situation in the metal oxide reagent. Indeed, barium is a very low electronegative cation forming very ionic bonds with oxygen anions; then, from an antagonist bond effect, the associated transition metal (M) is stabilized in ternary BaM_xO_y oxides with high oxidation state in order to form strongly covalent M–O bonds. In conclusion, changing the carbonate/oxide ratio in the initial mixture allows the formed phases to be varied with the consequent changes on the decarbonatation temperature and the characteristics of the color change (color, intensity, range).

Among the A, B and C mixtures, mixture B seems to be the best compromise for thermochromic applications. Indeed, introducing 80 wt% of barium carbonate and 20 wt% of hematite enables intense colors to be obtained (deep red and black), a reduced color change range (around 200 °C) and a quasi-unique formed phase $BaFeO_{3-x}$. 80: 20 carbonate: oxide ratio has been chosen as reference ratio for the following detailed studies.

A thermogravimetric analysis of mixture B (Fig. 2) illustrates a beginning of weight loss from 750 °C with an acceleration of the mass loss around 850 °C. According to the composition of the initial mixture (one oxide, one carbonate, no water) and the knowledge of the formed phase ($BaFeO_{3-x}$) thanks to X-ray diffraction analysis, this phenomenon can only be attributed to the decarbonatation reaction. The inset temperature (850 °C) of the weight loss corresponds to the color change of the mixture.

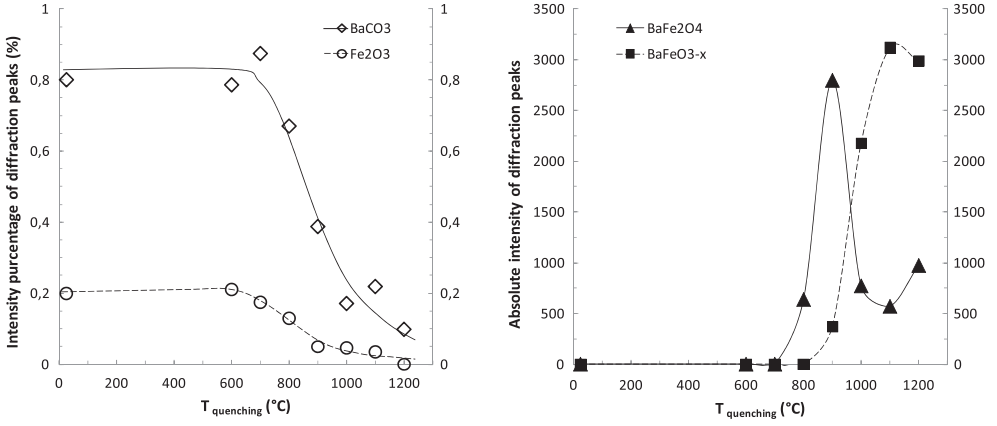

Fig. 4. Content evolution after semi-quantification of the mixed oxides issued from the decarbonatation reaction of the B mixture versus annealing temperature.

Powder X-ray diffractograms recorded on quenched mixtures from annealing temperatures ranging between 700 °C and 1200 °C (Fig. 3) point out the evolution of the reagents and the product phases content versus temperature. After annealing at 700 °C, only $BaCO_3$ and Fe_2O_3 reagents appear on the diffractogram showing that any reaction between the carbonate and the oxide has occurred in accordance with the thermogravimetric analysis. The decarbonatation reaction begins at 800 °C and is associated with the formation of $BaFe_2O_4$; then at 900 °C, the formation of $BaFeO_{3-x}$ takes place; at 1100 °C traces of $BaFe_4O_7$ oxides and at 1200 °C, traces of $BaFe_{12}O_{19}$ oxides are also detected. From a quantitative point of view, we have estimated the relative proportion of $BaCO_3$, Fe_2O_3, $BaFe_2O_4$ and $BaFeO_{3-x}$ phases from the main peak intensity of each phase on the X-ray diffractograms (Fig. 4). Whatever the mixture, thermal treatments over 800 °C induce a disappearance of the $BaCO_3$ and Fe_2O_3 reagents in favor of the formation of mixed oxides. One surprising point is the first appearance of $BaFe_2O_4$ compound at 700 °C followed by its disappearance around 1000 °C to the benefit of the perovskite $BaFeO_3$ type-form.

3.2. Extension to various $BaCO_3$–M_yO_x mixtures

The study performed on hematite allowed an understanding of the mechanism of the decarbonatation reaction between one carbonate and one oxide. Based on these results, the study was extended to other oxides with the aim to reach more detectable temperatures. Numerous binary and ternary oxides were directly annealed at high temperature (1200 °C) in order to focus only on those presenting a drastic color change between the starting mixture with $BaCO_3$ and the annealed mixture. Table 3 illustrates the evolution of the color of the mixture using various solid oxides versus annealing temperature. On the basis of the results obtained with hematite, all of the following mixtures were composed of 80 wt% of barium carbonate and 20 wt% of binary/ternary oxide.

At room temperature, the tested mixtures offer a wide range of colors: cream, dark red, pink, blue, green, grey or orange aspects are obtained. Each mixture exhibits different decarbonatation temperatures depending on the oxide reagent used. Indeed, decarbonatation temperatures T_D (temperature of the decarbonatation beginning) range from 400 °C to 1000 °C (Table 4). Moreover, the color change can be more or less sharp versus temperature. For example, mixture E containing $CoAl_2O_4$ as additive oxide has a sudden color change from dark blue to dark grey in the temperature range between 800 °C and 900 °C, while mixture $BaCO_3$–WO_3 changes progressively from pastel green to cream from 500 °C up to 1000 °C.

X-ray diffraction analyses were performed on all of the mixtures of the Table 3 after an annealing at 1100 °C in order to identify the main phases formed. The various phases detected are reported in the Table 4. The annealing of some mixtures lead to a unique phase formed. However, the annealing of others leads to the formation of at least three phases.

3.3. Predictive model to decarbonatation temperature from Er_3 calculation

In order to establish a predictive model allowing a rough prediction of the thermochromic decarbonatation, numerous approximations have been performed. Any reaction temperature is controlled by its reaction energy. Considering reaction (2), it can be obviously approximated that Er_1, Er_2 and Er_3: the reticular energies of the starting carbonate, the starting metal oxides and the main mixed oxide formed, respectively, take a major role comparing to ΔG_f formation of the CO_2 gas. Moreover, the ΔG_f formation of the

Table 3
Representation of the color of several decarbonatation mixtures after quenching at various temperatures between 400 °C and 1100 °C; calculation of the optical contrast (OC) and identification of the decarbonatation temperature (T_D); every decarbonatation reaction operates between 80% wt $BaCO_3$ and 20% wt oxide.

Oxide reagent	25°C	OC	500°C	OC	600°C	OC	700°C	OC	800°C	OC	900°C	OC	1000°C	OC	1100°C
$CuMoO_4$	63.8 9.1 15.7	15.8	52.8 -0.5 21.56	17.3	37.8 5.7 15.34	20.8	20.0 2.5 5.1	3.5	17.6 1.8 2.6	1.1	16.7 1.2 3.0	5.1	20.6 0.7 -0.2		
$CoAl_2O_4$	63.3 11.5 -17.8								33.45 -7.1 -8.5	17.1	23.9 1.3 2.9	7.4	16.7 0.8 1.7	3.9	15.1 -1.4 4.5
Fe_2O_3	38.3 28.0 18.3				40.2 26.8 16.3		40.0 27.6 17.4		39.5 27.8 24.6	29.5	33.6 2.7 10.3	17.9	18.9 -0.1 0.4	0.7	19.6 -0.3 0.2
ZnO:Co	77.0 -11.1 5.1						44.7 -6.2 6.4		39.8 -2.7 6.1	2.9	41.3 -1.8 3.9	19.2	60.5 -2.3 2.6	22.7	38.7 -3.1 8.9
NiO	81.4 -0.3 -0.1										49.8 0.6 2.6	24.2	25.8 2.1 5.1	2.4	28.2 2.1 5.1
$Y_2Ti_2O_7$	87.1 5.4 13.8						66.2 7.6 17.5	9.7	56.5 7.3 16.5	3.3	53.2 7.2 16.4	10.8	56.9 8.3 26.5	15.2	48.5 6.3 14.0
WO_3	89.4 -6.0 14.9	1.1	88.4 -6.1 14.6	2.1	88.8 -4.9 12.9	10.5	92.2 -0.8 3.8	1.5	92.0 0.1 2.7	1.7	90.7 0.2 3.8	1.4	89.4 -0.1 4.2	6.6	83.2 -0.2 6.6
Bi_2O_3	92.0 -2.5 8.4	2.9	91.6 -2.7 11.2	1.4	90.8 -1.6 11.7	22.0	70.8 -1.1 2.7	14.8	56.2 0.3 0.5	12.4	43.9 0.7 1.6	4.2	39.78 0.4 2.2		
V_2O_5	74.1 6.0 38.0	33.3	81.8 2.6 5.8	9.8	91.1 -0.5 5.3	1.5	91.5 -0.3 3.9	1.2	90.4 -0.5 4.3	0.4	90.0 -0.6 4.3	3.1	87.1 -0.4 5.3		
Cr_2O_3	55.3 -11.6 12.7	0.7	55.9 -11.3 12.6	2.3	57.7 -11.9 14.0	5.2	62.1 -12.7 16.7	23.6	80.5 -13.1 31.4	6.6	84.2 -12.1 36.8	33.9	58.4 -12.5 15.0		

Table 4
Identification of mixed oxides obtained after quenching from 1200 °C; Determination of the Bravais lattice of the main mixed oxide and calculation of its Er_3 reticular energy using the ionic model from Born.

	T_D (°C)	Mixed oxide (1200 °C)	ICDD file N°	Reference	Er_3 (kJ/mol)
D	550 °C	$BaMoO_4$ (100%)	01-089-4570	[14]	31,085
E	850 °C	$BaAl_2O_4$ (54%)	01-072-0387	[15]	21,870
		$Ba_6Co_4O_{12}$ (38%)	–	–	–
		$BaCoO_{2.5+x}$(8%)	–	–	–
B	850 °C	$BaFeO_{3-x}$	00-023-1024	[16]	12,605
		$BaFe_4O_7$	–	–	–
		$BaFe_2O_4$	–	–	–
		$BaFe_{12}O_{19}$	–	–	–
F	950 °C	$BaCoO_{3-x}$ (100%)	00-047-0211	[17]	~12,500
H	950 °C	$BaNiO_{2.5-x}$ (100%)	00-072-0405	[18]	~12,500
J	650 °C	Ba_3WO_6 (84%)	00-033-0182	[19]	38,220
		Ba_2WO_5 (12%)	–	–	–
		$BaWO_4$ (4%)	–	–	–
K	650 °C	$Bi_4Ba_{12}O_{22-x}$ (100%)	00-080-1492	[20]	33,660
L	450 °C	$Ba_3V_2O_8$ (95%)	00-029-0211	[21]	51,060
		$BaV_{13}O_{18}$ (5%)	–	–	–
M	750 °C	$BaCrO_4$ (70%)	00-035-0642	[22]	29,895
		$Ba_3Cr_2O_8$ (30%)	–	–	
N	1360 °C	BaO	00-061-6005	[23]	3505

CO_2 gas is the same for each decarbonatation reaction. Every mixture has been prepared using the same carbonate ($BaCO_3$), thus Er_1 is constant. Furthermore, in first approximation, the lattice binding energy of the formed mixed oxide can be considered as higher than the one of the simple starting oxide, BaO oxide being poorly stable; Er_2 can be minimized face to Er_3. Consequently, for all mixtures, the prediction of the energy of the decomposition reaction, i.e. the prediction of the decarbonatation temperature, can only be linked to the Er_3 reticular energy. A systematic calculation of the Madelung energy of the main phase characterized by X-ray diffraction analyses after annealing at 1100 °C will be proposed in order to be correlated to the experimental decarbonatation temperatures obtained by color change.

In Table 4, the ICDD files references (structural description of a crystalline phase), corresponding to the main oxide phases obtained after the annealing at 1100 °C are reported. These ICDD data were used to determine the Er_3 reticular energy. The Er_3 calculated values from our Ewald summation software are reported in the last column of Table 4. For comparison, the reticular energy of the BaO simple oxide is also presented; the corresponding decomposition temperature (T_D) was obtained from the literature [10].

The correlation curve between the calculated Er_3 energies and the experimental decarbonatation temperature is reported in Fig. 5. A negative correlation between these two parameters ($R^2 = 0.82$) is brought to the fore since while the Er_3 energy increases, the decarbonatation temperature decreases. Despite the numerous approximations made: the consideration of the main phase reticular energy only (e.g. the impact of the reticular energy of BaO being neglected), the direct correlation between reaction temperature and Er_3 energy can be considered as an acceptable key in order to establish a predictive model. Nevertheless, it is difficult to determine the reticular energy for complex oxide structures. It is for this reason that to go further a predictive approach which associates the decarbonatation temperature to other simple parameters has been proposed.

Based on a solid-state chemistry approach of mixed oxide, one can think that the most stable mixed oxide formed with Ba^{2+}, which is a very low electronegative cation, are composed with electronegative

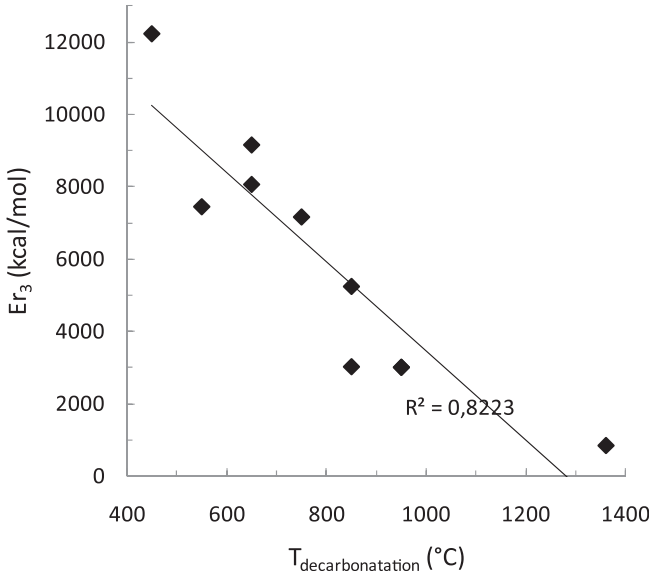

Fig. 5. Correlation between Er_3 reticular energy and T_D decarbonatation temperature.

B^{n+} cations due to the stabilization of bonds all the more ionic than they are adjacent to covalent bonds (antagonist bond effect). Hence, a correlation between the electronegativity of the B^{n+} cation and the Er_3 reticular energy was expected. The electronegativity values of the B^{n+} cations (according to the Sanderson scale [9]) are reported in Table 5. From these data, the decarbonatation temperature curve of $BaCO_3/B^{n+}$ oxide mixtures versus the B^{n+} electronegativity values was plotted (Fig. 6). One can see the correlation reliability factor is very low, showing a poor correlation between the B^{n+} electronegativity and decarbonatation temperatures.

Brown [12,13] has explained the importance of bond valences in oxides and gives a list of ideal coordination numbers (i.c.n.) for all the cations, this list being based on the average coordination number (n) observed for each cation and the oxygen anion from a multitude of compositions: i.c.n. is an empiric factor. In mixed oxides, in a predictive way, the stability of a solid crystal is linked to the coordination number of the cations/anions inside the structure: the closer the coordination numbers of the cations/anions are to their i.c.n., the more stable a crystalline oxide (lower its reticular energy). For a cation, the ratio of its oxidation degree (d.o.) on its i.c.n. value leads to an estimation of the cation bond strength (b.s) which represents the most probable (ideal) valence of the bonds formed by the cations. For the oxygen anion in solid oxides, the b.s. value is 0.5: the i.c.n. being 4 (tetrahedral coordination) and the

Table 5
Electronegativity (Sanderson), i.c.n.: ideal coordination number, n: oxidation degree and bonding strength of B^{n+} cation.

	Main mixed oxide formed	B^{n+}	B^{n+} electronegativity	B^{n+} i.c.n.	B^{n+}n	B^{n+} bonding strength
D	$BaMoO_4$	Mo^{6+}	2.20	4.9	6	1.22
E	$BaAl_2O_4$	Al^{3+}	1.71	5.27	3	0.57
B	$BaFeO_{3-x}$	Fe^{3+}	2.20	5.70	3	0.53
F	$BaCoO_{3-x}$	Co^{3+}	2.56	5.9	3	0.51
G	Ba_3WO_6	W^{6+}	1.67	5.6	6	1.07
H	$BaNiO_{2,36}$	Ni^{2+}	1.94	5.9	2	0.34
J	Ba_3WO_6	W^{6+}	1.67	5.6	6	1.07
K	$Bi_4Ba_{12}O_{21,92}$	Bi^{5+}	2.34	6.2	5	0.81
L	$Ba_3V_2O_8$	V^{5+}	2.51	4.6	5	1.09
M	$BaCrO_4$	Cr^{6+}	3.37	4.0	6	1.50
N	BaO	Ba^{2+}	0.68	10.2	2	0.20

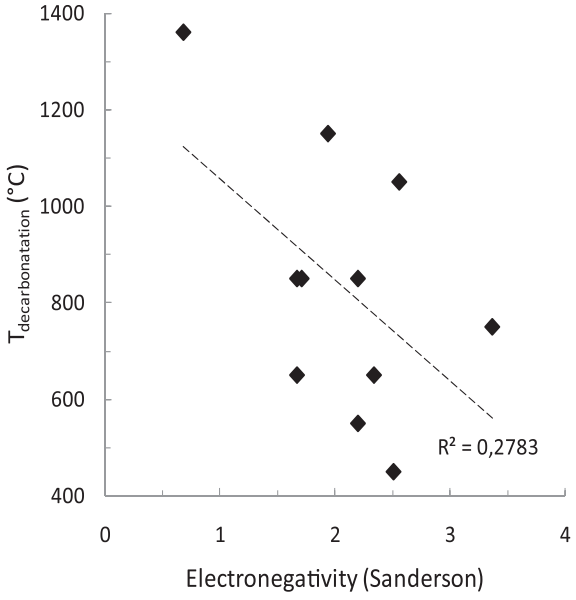

Fig. 6. Decarbonatation temperature versus B^{n+} Sanderson electronegativity.

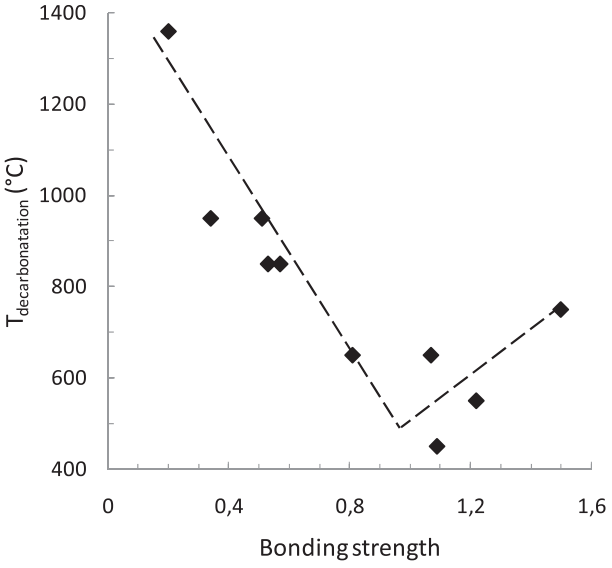

Fig. 8. Decarbonatation temperature versus B^{2+} bonding strength.

oxygen oxidation degree -II. For the barium cation, the b.s. value is 0.2: the i.c.n. being 10 and the oxygen oxidation degree -II. So as the oxygen anion is linked to cations like Ba^{2+}, the b.s. of the Ba-O bonds cannot be satisfying for both elements. The Ba^{2+} bond strength in an oxide (0.2) is largely lower to the O^{2-} one: 0.5. Hence, in Ba—O oxides, barium and oxygen ions exhibit unsatisfying coordination numbers, too low for barium and to high for oxygen. Therefore, in order to respect the matching valence principle [12], the ternary barium-metal oxides will be all the more stable than the metal counter cation possesses a high b.s. In Fig. 7, is reported the ideal arrangement around the oxygen in barium-metal mixed oxides. The ideal structural arrangement is considered as the one respecting the i.c.n of the oxygen anion (equal to 4). One can see that in the ideal case, the transition metal B^{n+} has to exhibit a relatively high bond strength value: equal to 0.8, in the optimal case. The decarbonatation temperature and the b.s. of the B^{n+} cation were finally correlated. The b.s. values are compiled in Table 5. The correlation curve between decarbonatation temperature T_D and the B^{n+} b.s. value is plotted in the Fig. 8. The as-established correlation is obviously negative for b.s. values inferior to 0.8 and positive for b.s. values superior to 0.8, i.e. the 0.8 critical bond strength corresponds well on the graph to the minimal decarbonatation temperature, i.e. the mixed oxides formed are in first approximation the most stable on this critical point.

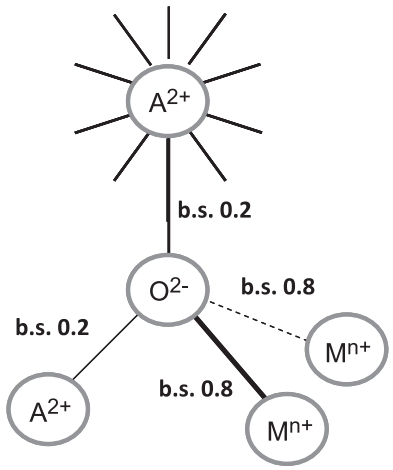

Fig. 7. Schematic representation of an ideal $Ba_1M_1O_z$ mixed oxide, i.e. according to the bonding strength and ideal coordination numbers for Ba and O atoms.

4. Conclusion

Thermochromic mixtures based on a barium carbonate and the addition of a metal transition oxide allow indicating a wide range of temperatures since a significant color change is associated to the decarbonatation and the formation of barium − transition metal mixed oxide. The difference in color between the reagent mixture and the formed mixed oxide is generally due to the increase of the oxidation state of the transition metal. Indeed, the barium is a very low electronegative cation forming very ionic bonds with oxygen anions; then, from antagonist bond effect (stabilization of structures with an alternation of ionic and covalent bonds), the associated transition metal (*M*) is stabilized in ternary BaM_xO_y oxides with a high oxidation state in order to form strongly covalent M—O bonds. The decarbonatation temperature, i.e. the thermochromic effect in an applicative point of view, can be rather well predicted from bond valence considerations. Here, using a barium carbonate as the main reagent, the counter cations chosen in the added metal oxides, have to exhibit a bonding strength around 0.8 in order to get the minimal decarbonatation temperature. This phenomenon constitutes an illustration of the matching valence principle enounced by Brown [13] which stated that ionic crystals are all the more stable when the bonding strength of the anions is close to the bonding strength of the cations. Hence, quasi-infinite possibilities combining further transition metal oxides and alkaline-earth carbonates can be easily achieved based on the carbonate-oxide mixtures studied in this paper in order to propose temperature indicators working between 400 and 1200 °C.

Acknowledgments

The “Direction Générale de l’Equipement” (DGE) is acknowledged for financial support through the ARTIQ consortium.

The authors would like to acknowledge ID Brown, "The Chemical Bond in Inorganic Chemistry" being our main source of inspiration.

References

[1] Gaudon M, Deniard P, Demourgues A, Thiry AE, Carbonera C, Le Nestour A, et al. Unprecedented "One-Finger-Push"-induced phase transition with a drastic color change in an inorganic material. Advanced Materials 2007;19:3517.

[2] Gaudon M, Carbonera C, Thiry AE, Demourgues A, Deniard P, Payen C, et al. Adaptable thermochromism in the $CuMo_{1-x}W_xO_4$ series $(0 \leq x < 0.1)$: a behavior related to a first-order phase transition with a transition temperature depending on x. Inorganic Chemistry 2007;46:10200.

[3] Popescu M, Serban L, Popescu M. Thermo-indicating paint for damage warning. Journal of Thermal Analysis 1996;46:317–21.

[4] European patents EP1288266A1-EP1614724A2, Inv:Watson HML, Owner:-Rolls-Royce.

[5] European Patents EP1291394A1, EP1291395A1, EP1288267A1, Inv:Watson HML, Hodgkinson EC, Owner:Rolls-Royce.

[6] S. Somani. Chromic materials, phenomena and their technological applications. Applied Science Innovations Privite Limited, Ed., 2010.

[7] Day JH. Thermochromism of inorganic compounds. Chemical Reviews; 1968:68–76.

[8] Nassau K. The physics and chemistry of color, the fifteen causes of color. 2nd ed. New York: Wiley; 2001.

[9] Huheey JE, Keiter EA, Keiter RL. Chimie inorganique. Paris: De Boeck Université; 1996.

[10] Handbook of chemistry and physics. 56th ed. CRC Press; 1975–1976.

[11] Ewald PP. The calculation of optical and electrostatic grid potential. Annals of Physics 1921;64:253.

[12] Brown ID. The chemical bond in inorganic chemistry, the bond valence model. Oxford: Science Publications; 2002.

[13] Brown ID, Altermatt D. Acta Crystallographica 1985;B41:244.

[14] Nassif V, Carbonio RE, Alonso JA. Neutron diffraction study of the crystal structure of BaMoO4: a suitable precursor for metallic $BaMoO_3$ perovskite. Journal of Solid State Chemistry 1999;146:266–70.

[15] Perrotta AJ, Smith JV. Crystal structure of $BaAl_2O_4$. Bulletins de la Société Française de Minéralogie et Cristallographie 1968;91:85.

[16] Negas T, Roth RS. Synthesis of barium ferrates in oxygen. Journal of Research, National Bureau of the Standards, Section A 1969;73:425.

[17] Jacobson AJ, Hutchison JL. An investigation of the structure of $^{12H}BaCoO_{2.6}$ by electron-microscopy and powder neutron diffraction. Journal of Solid State Chemistry 1980;35:334–40.

[18] Krischne H, Torkar K, Kolbesen BO. System BaO–NiO. Journal of Solid State Chemistry 1971;3:349–57.

[19] Steward EG, Rooksby HP. Pseudo-cubic alakaline-earth tungstates and molybdates of the R_3MX_6 type. Acta Crystallographica 1951;4:503.

[20] Licheron M, Gervais F, Coutures J, Choisnet J. Ba_2BiO_4 surprisingly found as a cubic double perovskite $Ba_2(Ba_{2/3}Bi_{1/3})BiO_6$-sigma. Solid State Communications 1990;75:759–63.

[21] Liu G, Greedan JE. Syntheses, structures and characterization of 5-layer $BaVO_{3-x}$ ($x = 0.2, 0.1, 0.0$). Journal of Solid State Chemistry 1994;110:274–89.

[22] Hauff P, Foord EE, Rosenblum S, Hakki W. Hashemite Ba(Cr, S)O_4, a new mineral from Jordan. American Mineralogist 1983;11-12:1223–5.

[23] Taylor D. Thermal-expension data.1. Binary oxides with the sodium-chloride and wurtzite structures, MO. Transactions and Journal of the British Ceramic Society 1984;83:5.